Activation Energy for Mobility of Dyes and Proteins in Polymer Solutions: From Diffusion of Single Particles to Macroscale Flow

Krzysztof Sozański, Agnieszka Wiśniewska, Tomasz Kalwarczyk, and Robert Hołyst*

Institute of Physical Chemistry, Polish Academy of Sciences, Kasprzaka 44/52, 01-224 Warsaw, Poland

(Received 21 May 2013; revised manuscript received 7 August 2013; published 26 November 2013)

We measure the activation energy E_a for the diffusion of molecular probes (dyes and proteins of radii from 0.52 to 6.9 nm) and for macroscopic flow in a model complex liquid—aqueous solutions of polyethylene glycol. We cover a broad range of polymer molecular weights, concentrations, and temperatures. Fluorescence correlation spectroscopy and rheometry experiments reveal a relationship between the excess of the activation energy in polymer solutions over the one in pure solvent ΔE_a and simple parameters describing the structure of the system: probe radius, polymer hydrodynamic radius, and correlation length. ΔE_a varies by more than an order of magnitude in the investigated systems (in the range of ca. 1–15 kJ/mol) and for probes significantly larger than the polymer hydrodynamic radius approaches the value measured for macroscopic flow. We develop an explicit formula describing the smooth transition of ΔE_a from the diffusion of molecular probes to macroscopic flow. This formula is a reference for the quantitative analysis of specific interactions of moving nano-objects with their environment as well as active transport. For instance, the power developed by a molecular motor moving at constant velocity u is proportional to $u^2 \exp(E_a/RT)$.

DOI: 10.1103/PhysRevLett.111.228301 PACS numbers: 82.20.Pm, 47.57.eb, 47.57.Ng, 83.80.Rs

The rapid development of nanotechnology and bioengineering at the molecular level poses new requirements for an accurate and applicable description of mobility in complex systems. Much attention has been recently drawn to molecular motors—nanoscaled devices, converting energy (mostly chemical, e.g., stored in ATP) into mechanical work and motion [1]. The estimation of the amount of energy dissipated during the movement is the key for determining the efficiency of such motors [2]. The unresolved experimental problem is how to quantify the work exerted against the hydrodynamic drag and measure the dissipation at the nanoscale in complex liquids? The answer to this and different other questions arising in nanotechnology, biophysics, or fluid dynamics can be found by a careful analysis of the size-dependent hydrodynamic drag and the energy involved in the process of spontaneous diffusion.

The drag is connected with the diffusion coefficient by the fluctuation-dissipation theorem [3]. Pure diffusion can be treated as a reference for cases where extra energy (other than the energy of thermal motions) is expended. As was proven by Eyring, simple Brownian diffusion is an activated process, subject to the rate theory and Arrhenius law [4,5]. Consequently, the diffusion coefficient D of any given species in any given system is defined by a characteristic activation energy E_a. In general, the value of E_a should depend on the viscous and structural properties of the fluid and on the interactions of the probe with the surrounding entities. Both these factors are of great importance in biological systems, influencing, e.g., protein association [6] or repressor-operator binding rates [7]. In the crowded cellular environment, complex size effects [8], motion hindrance by significant interactions or fixed obstacles [9], as well as a variety of possible active transport mechanisms [10,11] including molecular motors [1] play important roles for cell functionality. To properly describe mobility in complex systems at the micro- and nanoscales and understand the underlying physics, the contribution of different factors to the overall diffusion rates must be identified. For that purpose, we propose to employ the notion of activation energy. We follow Eyring's approach, describing diffusion as a combination of single acts of translation of a molecule from one equilibrium state to an adjacent one [4,5]. This approach was merged with the free volume theory of Cohen and Turnbull [12] to include the probabilities of finding and moving into a hole in a particle's vicinity [13,14]. Although various ways of incorporating the temperature dependence into diffusion equations were suggested [15–18], they did not include structure-related factors that would allow for the scaling and direct application of the theory to polymer solutions and other complex liquids. On the other hand, most of the relevant polymer research is either focused on very specific cases, such as mobility in melts in the vicinity of the glass transition [19,20], or deals only with the macroscopic viscous flow [21–24]. The latter approach neglects the fact that probe diffusion and viscous flow can be described in a unified way.

According to the Stokes-Sutherland-Einstein (SSE) equation ($D = k_B T/6\pi\eta r_p$), diffusion rates depend on the probe radius r_p and solution viscosity η. Numerous studies disclosed severe violations of this relation in complex systems [25–30], demonstrating an apparent enhancement of diffusion rates of relatively small probes. The effect was also observed in HeLa [8] and *E. coli* [31] cells. Research on model polymer systems revealed that the

SSE relation holds only when the probe radius r_p exceeds the radius of gyration of the polymer coil R_g [29,30,32]. In our recent work, we demonstrated that the formula retains validity for the whole range of probe sizes and environments, on the condition that viscosity is treated as a variable, dependent on the scale of the flow around the probe [30,33]. The magnitude of this length-scale dependence can be vast: for instance, the macroscopic viscosity of a 3% polyethylene glycol ($M_w = 500$ kDa) aqueous solution is over 90 times higher than the viscosity experienced by a molecular probe (ca. 1 nm in diameter) diffusing in such solution. However, we did not find any literature record of a systematic analysis of the diffusion of various molecular probes in complex liquids as a function of temperature, which seems the obvious way to investigate the activation energy for mobility. A simple question that has not been answered so far is what is the difference between the E_a for the mobility of a small protein (or other given molecule) in a polymer solution and the E_a for the macroscopic flow of the same liquid? The length-scale dependence of E_a should provide a reference for the qualitative and quantitative analysis of other factors influencing the molecular mobility (association and complex formation or active transport). In this Letter, we give an explicit formula for E_a, pinpointing the influence of the geometry- and scale-related parameters.

Polymers and probes.—We investigated well-characterized complex liquids—aqueous solutions of polyethylene glycol (PEG)—over a wide range of molecular masses (3–500 kDa), concentrations (1%–30%), and temperatures (278–315 K). To eliminate the temperature dependence of solvent viscosity, we put all the results in terms of relative diffusion coefficients D/D_0, where D_0 is the diffusion coefficient of given species in water. To merge data on viscosity η and diffusion rates, we applied the relation [30]

$$\frac{D}{D_0} = \frac{\eta_0}{\eta}, \tag{1}$$

where η_0 refers to the viscosity of pure solvent (water) at given conditions [34].

Only semidilute polymer solutions were investigated. In this regime, the polymer concentration c exceeds the overlap concentration c^*, defined as

$$c^* = \frac{M_w}{4/3\pi R_g^3 N_A}, \tag{2}$$

where M_w is the polymer molecular weight, R_g is the polymer gyration radius, and N_A is the Avogadro number. In a good solvent, polymer chains do not form separate coils but interpenetrate each other, forming a loose mesh [35] characterized by a specific correlation length ξ, i.e., the average distance between points of entanglement of different chains. This length depends on the polymer concentration

$$\xi = R_g\left(\frac{c}{c^*}\right)^{\beta}, \tag{3}$$

where $\beta = -0.75$ [36]. ξ has already been used previously for quantitative description of scale-dependent viscosity, as $\ln\eta \propto r_p/\xi$ [37]. The polymer gyration and hydrodynamic radii, expressed in nanometers, can be calculated from empirical equations based on light scattering experiments [38]

$$R_g = 0.0215 M_w^{0.583}, \qquad R_h = 0.0145 M_w^{0.57}. \tag{4}$$

We used both regular, high-grade polymers and molecular weight standards. Actual molecular weights and their distributions were examined by gel permeation chromatography (Supplemental Material [39]), whereas in the text a simplified notation was used (e.g., PEG 20k denotes polyethylene glycol of number average molecular weight of ca. 20 kDa). In fluorescence correlation spectroscopy (FCS) experiments, we applied a range of probes of different hydrodynamic radii: fluorescent dyes, rhodamine B ($r_p = 0.57$ nm) and rhodamine 110 ($r_p = 0.52$ nm) as well as labeled proteins of chicken egg lysozyme ($r_p = 1.9$ nm) and horse spleen apoferritin ($r_p = 6.9$ nm). For protein labeling, we used Atto 488 and Atto 550 kits according to the suggested protocols. The solvent used in FCS measurements was phosphate buffer (pH = 7.0, NaCl added to maintain the physiological ionic strength), preserving the proteins in their native form and providing screening of electrostatic interactions.

Methods: rheometry.—The macroviscosity of PEG solutions was measured using a Malvern Kinexus rotational rheometer, in a temperature range of 278–323 K. The geometry of the measurement system was adjusted to the rheological properties of the sample. For low-viscosity samples (of the order of pure solvent viscosity), a double-cylinder geometry was used, whereas for high-viscosity samples a cone-plate system was applied. As the goal of the measurements was to establish the viscosity at zero shear rate, which was not directly possible, measurements were performed with precise control of the shear stress in the range of 0.01–10 Pa and then linear extrapolation was performed.

Methods: FCS.—We used FCS to investigate the mobility of fluorescent dyes and labeled proteins of radii ranging from 0.52 to 6.9 nm. FCS probes the average, long-time diffusion coefficients of single particles. To observe fluorescence fluctuations, the total displacement of probes during the experiment must be of the order of micrometers to significantly exceed the dimensions of the focal spot. However, the scale of local hydrodynamic flow coupled with the random movements of the probe in the solution is in the range of molecular dimensions (nanometers).

The FCS setups were comprised of commercial Nikon C1 and Nikon A1 inverted confocal microscopes, both coupled with complete time-correlated single photon counting systems from PicoQuant and water immersion

objectives Nikon PlanApo 60 ×, NA = 1.20. The main experimental problems and challenges were due to the distortions of the confocal volume by the difference in temperature with respect to ambient conditions and in refractive indices (RIs) of polymer solutions with respect to pure water. If not properly taken into account, both of these factors would preclude the quantitative determination of the excess activation energy. To precisely control the sample temperature and vary it in a possibly broad range without a substantial influence on the optical parameters of the setup, we designed a two-stage system [40]. Its working range was 278–315 K, with an accuracy of ±0.1 K. To resolve the issue of significant mismatch between the RI of the immersion liquid and the sample, we developed a method of relative data analysis. Every FCS experiment was repeated in identical conditions, except that instead of PEG a solution of monomolecular ethylene glycol of matching RI and known macroscopic viscosity was used. Since in the glycol solutions (where no macromolecules were present) the probes experienced viscosity matching the macroscopic value and the chemical surroundings of probes in both glycol and PEG solutions were very similar, such measurements provided a perfect reference. The relative analysis allowed us to minimize artifacts and systematic errors connected with the RI mismatch and assumption of the Gaussian profile of the confocal volume. Quantitative comparison of the results obtained for samples differing in RI was therefore possible. Further details on the applied FCS experimental methods are available in the Supplemental Material [41].

Results and discussion.—Although a significant part of the temperature dependence of viscosity came from the changes in the solvent viscosity, the decrease of relative viscosity with increasing temperature was accurately captured in our experiments. Relation 1 was applied to present the results in terms of relative diffusivity. From the shape of the curves, a simple dependence of $1/T$ type could be inferred (exemplary data available in the Supplemental Material [42]). This was in line with the predictions concerning an Arrhenius-type dependence in the formula for relative diffusivity, based on the Eyring equations [5]. This approach was combined with the description of viscosity of polymer systems introduced in our earlier work [30,33], based on a logarithmic dependence of relative viscosity on $(R_h/\xi)^a$. Parameter a in analogous equations may vary from system to system, whereas its physical meaning is still under discussion [43]. We established it by means of a separate, ample set of experimental data for PEG solutions (Supplemental Material [42]). The value of a used for further calculations was 0.78. All the rheometry data were plotted against $(R_h/\xi)^a(RT)^{-1}$ (Fig. 1). The results for all the PEG solutions, presented in Fig. 1, fell onto one linear curve, regardless of the molecular weight of the polymer or its concentration. Tests performed by means of dynamic light scattering revealed no significant changes in the R_h of the polymers with temperature within the measurement range (Supplemental Material [44]). The

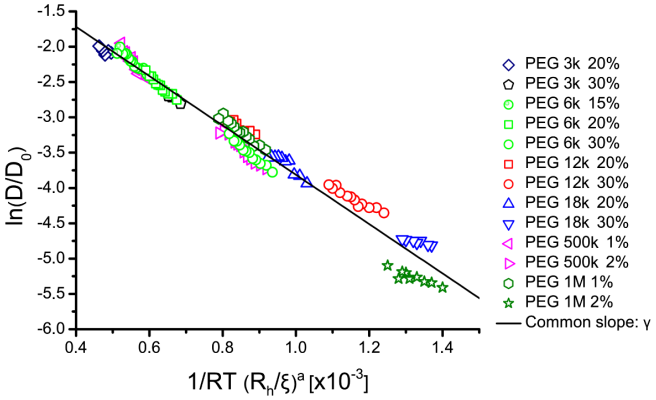

FIG. 1 (color online). Relative diffusivity at the macroscale for different PEG solutions plotted according to the proposed scaling equation. The slope of the concentrate linear fit corresponds to the coefficient γ [see Eq. (5)], equal to ca. 3.96 kJ/mol.

slope of the curves obtained from the macroscale experiments is a constant γ, expressed in terms of energy and equal 3.96 ± 0.40 kJ/mol. The error here is given as a maximum discrepancy between the results for fits of individual data sets; γ is characteristic for the system (in this case, PEG/water) and does not depend on either the polymer concentration or molecular mass. Thus, the diffusion coefficient for large objects ($r_p \gg R_h$) is given by

$$D = D_0 \exp\left[\frac{-\gamma(R_h\xi^{-1})^a}{RT}\right]. \quad (5)$$

Macroscopic viscous flow of a polymer solution is also described by Eq. (5) due to the reverse dependence of relative viscosity and diffusivity [Eq. (1)].

We performed FCS measurements to prove that this kind of dependence can be transferred to the mobility of nanoscaled probes. In this case, probe radius r_p became an additional variable. We used the notion of effective radius defined previously [33] as

$$R_{\text{eff}}^{-2} = R_h^{-2} + r_p^{-2}. \quad (6)$$

The logarithm of the relative diffusivity measured for the molecular probes also depended reciprocally on the temperature. Diffusivity scaling was included analogously as at the macroscale, using R_{eff} instead of R_h. Such an approach was justified, as the macroscopic flow was the limiting case for the scaling we postulated: $\lim_{r_p\to\infty} R_{\text{eff}} = R_h$. For each probe-polymer system, all the results fell along a straight line on the scaling plot (Fig. 2). Therefore, Eq. (5) could be rewritten to include scaling with the probe and polymer chain sizes as

$$D = D_0 \exp\left[\frac{-\gamma(R_{\text{eff}}\xi^{-1})^a}{RT}\right]. \quad (7)$$

The obtained results and their proposed description proved fully consistent with the viscosity scaling we postulated in our previous work [30,33]. By analogy to the original Eyring rate theory, the denominator in Eq. (7)

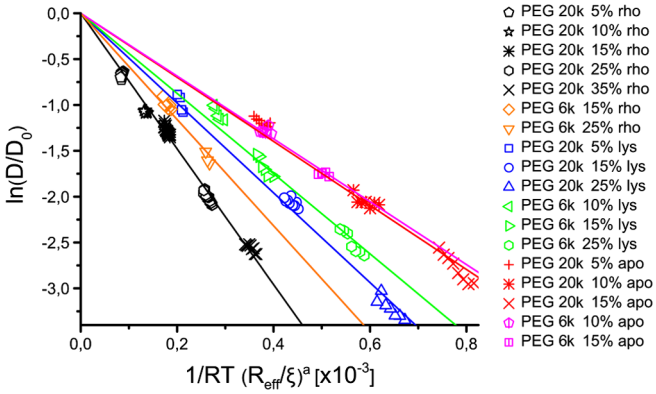

FIG. 2 (color online). Relative diffusivity experienced by molecular probes in PEG solutions plotted according to the proposed scaling equation. Probe descriptions: rho, rhodamine ($r_p = 0.52$ nm); lys, lysozyme ($r_p = 1.9$ nm); apo, apoferritin ($r_p = 6.9$ nm).

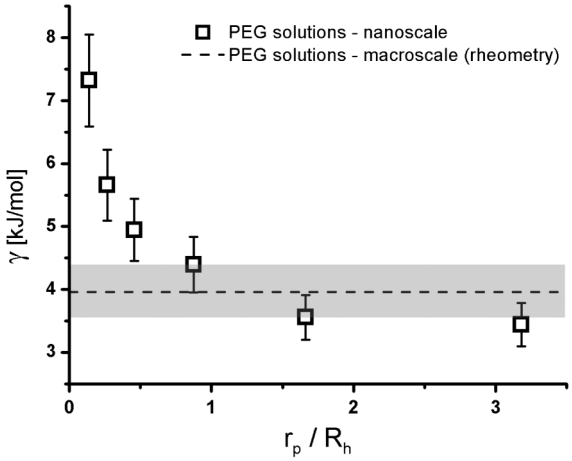

FIG. 3. Dependence of the γ coefficient [Eqs. (7) and (8)] on the probe/polymer size ratio. Relatively large molecular probes reproduce well the results of macroviscosity measurements. The shaded range denotes the maximal error of rheometry results.

was interpreted as the excess of activation energy for diffusion over the value characteristic for pure solvent, giving

$$\Delta E_a = \gamma\left(\frac{R_{\mathrm{eff}}}{\xi}\right)^a. \tag{8}$$

The FCS results matched the proposed scaling of relative viscosity (Fig. 2) very well. However, contrary to the macroscopic case, significant differences in the obtained γ values were observed between different probe-polymer systems. The changes were systematic and corresponded to the transition from the macro- to nanoviscosity range, as shown in Fig. 3. For systems characterized by $r_p/R_h > 1$, the values of γ coefficient obtained from FCS experiments approached a constant and reproduced the macroscopic value well (within experimental errors). This supports both the high quality of the obtained results and the postulated identity in the description of viscous flow and probe diffusion. In the $r_p/R_h > 1$ range, the probe gradually starts to experience the macroscopic viscosity of the solution [33]. This smooth shift is manifested by changes in both the relative diffusion coefficient D/D_0 and the excess activation energy ΔE_a, and an exemplification can be found in Table I.

In this Letter, we focused on the notion of activation energy for the movement of a probe in a polymer solution. We measured and described the excess of E_a over the value characteristic for the pure solvent for different molecular probes as well as for the macroscopic flow. We have proven that the activation energy for diffusion in polymer solutions depends on the structure of the system [Eq. (7)]. When probe size increases above the hydrodynamic radius of the polymer chain, ΔE_a reaches a limit, corresponding to the value measured for the macroscopic flow. For instance, the value of ΔE_a calculated for rhodamine in 3% PEG 500k solution (small probe, long polymer chains) is ca. 1.1 kJ/mol, for appoferritin (larger probe) it reaches 6.3 kJ/mol, whereas for macroscopic flow ΔE_a is ca. 12 kJ/mol. As has been shown previously, mobility scaling equations can be transferred from PEG solutions to other complex liquids, such as micellar systems or even living cell cytoplasm [33]. In cytoplasm, the mobility of macromolecules is mostly influenced by high concentration of proteins [46] as well as by the presence of the DNA [47] and cytoskeleton [48]. All these physical "obstacles" can be included in the simplified geometric description of the structure of the complex liquid, allowing for the application of the scaling equation to such systems. Significant increase of ΔE_a value over the one predicted by the presented benchmark formula should imply molecular association processes, hindering the motion. On the other hand, molecular traffic in cells is in fact an interplay between spontaneous diffusion and active transport [49]. The work exerted in the active process can be inferred from the comparison of the measured and predicted (for the purely Brownian motion) ΔE_a values. Confrontation of the work done with the total amount of energy used for the motion enhancement (which can be monitored, e.g., via ATP usage in a number of enzyme-based systems [50]) should enable

TABLE I. Excess of the activation energy over the one in pure water, ΔE_a; exemplary data for PEG aqueous solutions ($M_n = 20$ kDa). D_0 refers to diffusion in pure water. The activation energy for the self-diffusion of water is 19 kJ/mol [45]. According to Eq. (1), relative diffusivity is an inverse of relative viscosity, which is how the reference values for macroscopic flow are calculated.

Probe, r_p [nm]	Concentration [%]	D/D_0 at 298 K	ΔE_a [kJ/mol]
Rhodamine, 0.5	10	0.34	2.50
Lysozyme, 1.9		0.30	4.04
Apoferritin, 6.9		0.13	5.17
Macroscopic flow		0.077	6.37
Rhodamine, 0.58	25	0.13	4.87
Lysozyme, 1.9		0.038	7.87
Macroscopic flow		0.0067	12.4

the determination of the intrinsic energy dissipation, which in turn allows for an estimation of the molecular motor efficiency. Furthermore, application of the fluctuation-dissipation theorem and Stokes' law leads to a dependence between E_a and the power P of a motor moving at a constant velocity u: $P \propto u^2 \exp(E_a/(RT))$. Utilization of the notion of activation energy for mobility in complex liquids may therefore provide new insight into the description of molecular transport—both passive and active—and enable better understanding and modeling of dynamic processes in any kind of diffusion-controlled systems.

T. K. and K. S. thank the Ministry of Science of Poland for support within the Iuventus Plus program IP2011 021771. R. H. thanks the National Science Center for funding the project from the funds granted on the basis of decision number 2011/02/A/ST3/00143 (Maestro grant). This work was done in the NanoFun laboratories founded by POIG.02.02.00-00-025/09.

*rholyst@ichf.edu.pl

[1] P. Haenggi and F. Marchesoni, Rev. Mod. Phys. **81**, 387 (2009).
[2] Y. Zhang, J. Stat. Phys. **134**, 669 (2009).
[3] R. Kubo, Rep. Prog. Phys. **29**, 255 (1966).
[4] H. Eyring, J. Chem. Phys. **4**, 283 (1936).
[5] R. E. Powell, W. E. Roseveare, and H. Eyring, Ind. Eng. Chem. **33**, 430 (1941).
[6] M. Tabaka, L. Sun, T. Kalwarczyk, and R. Hołyst, Soft Matter **9**, 4386 (2013).
[7] J. Elf, G.-W. Li, and X. S. Xie, Science **316**, 1191 (2007).
[8] G. L. Lukacs, P. Haggie, O. Seksek, D. Lechardeur, N. Freedman, and A. S. Verkman, J. Biol. Chem. **275**, 1625 (2000).
[9] J. A. Dix and A. Verkman, Annu. Rev. Biophys. **37**, 247 (2008).
[10] C. Loverdo, O. Benichou, M. Moreau, and R. Voituriez, Nat. Phys. **4**, 134 (2008).
[11] S. C. Weber, A. J. Spakowitz, and J. A. Theriot, Proc. Natl. Acad. Sci. U.S.A. **109**, 7338 (2012).
[12] D. Turnbull and M. H. Cohen, J. Chem. Phys. **52**, 3038 (1970).
[13] P. B. Macedo and T. A. Litovitz, J. Chem. Phys. **42**, 245 (1965).
[14] G. Han, Z. Fang, and M. Chen, Sci. China Phys. Mech. Astron. **53**, 1853 (2010).
[15] A. C. Fernandez and G. D. J. Phillies, Biopolymers **22**, 593 (1983).
[16] I. Avramov, Phys. Chem. Glasses B **48**, 61 (2007).
[17] S. Morioka and M.-H. Sun, J. Non-Cryst. Solids **355**, 287 (2009).
[18] J. S. Vrentas and J. L. Duda, J. Polym. Sci. Polym. Phys. Ed. **15**, 417 (1977).
[19] T. Inoue, M. T. Cicerone, and M. D. Ediger, Macromolecules **28**, 3425 (1995).
[20] M. T. Cicerone, F. R. Blackburn, and M. D. Ediger, Macromolecules **28**, 8224 (1995).
[21] P. Flory, J. Chem. Phys. **13**, 453 (1945).
[22] G. Berry and T. Fox, *The Viscosity Of Polymers and Their Concentrated Solutions*, Advances in Polymer Science, Vol. 5 (Springer-Verlag, Berlin, 1968), p. 261.
[23] L. T. Novak, C. C. Chen, and Y. Song, Ind. Eng. Chem. Res. **43**, 6231 (2004).
[24] R. Sadeghi, J. Chem. Thermodyn. **37**, 445 (2005).
[25] H. K. Schachman and W. F. Harrington, J. Am. Chem. Soc. **74**, 3965 (1952).
[26] G. D. J. Phillies, G. S. Ullmann, K. Ullmann, and T. H. Lin, J. Chem. Phys. **82**, 5242 (1985).
[27] F. Brochard-Wyart and P. G. de Gennes, Eur. Phys. J. E **1**, 93 (2000).
[28] J. Szymanski, A. Patkowski, A. Wilk, P. Garstecki, and R. Holyst, J. Phys. Chem. B **110**, 25593 (2006).
[29] A. Tuteja, M. E. Mackay, S. Narayanan, S. Asokan, and M. S. Wong, Nano Lett. **7**, 1276 (2007).
[30] R. Hołyst, A. Bielejewska, J. Szymański, A. Wilk, A. Patkowski, J. Gapiński, A. Zywociński, T. Kalwarczyk, E. Kalwarczyk, M. Tabaka, N. Ziębacz, and S. A. Wieczorek, Phys. Chem. Chem. Phys. **11**, 9025 (2009).
[31] M. B. Elowitz, M. G. Surette, P. E. Wolf, J. B. Stock, and S. Leibler, J. Bacteriol. **181**, 197 (1999).
[32] J. Liu, D. Cao, and L. Zhang, J. Phys. Chem. C **112**, 6653 (2008).
[33] T. Kalwarczyk, N. Ziębacz, A. Bielejewska, E. Zaboklicka, K. Koynov, J. Szymański, A. Wilk, A. Patkowski, J. Gapiński, H.-J. Butt, and R. Hołyst, Nano Lett. **11**, 2157 (2011).
[34] E. Lemmon, M. Mclinden, and D. Friend, *NIST Chemistry Webbook, NIST Standard Reference Database Number 69* (National Institute of Standards and Technology, Gaithersburg, MD, 2012).
[35] P.-G. de Gennes, *Scaling Concepts In Polymer Physics* (Cornell University Press, Ithaca, 1979).
[36] Y. Cheng, R. K. Prud'homme, and J. L. Thomas, Macromolecules **35**, 8111 (2002).
[37] D. Langevin and F. Rondelez, Polymer **19**, 875 (1978).
[38] K. Devanand and J. C. Selser, Macromolecules **24**, 5943 (1991).
[39] See the Supplemental Material at http://link.aps.org/supplemental/10.1103/PhysRevLett.111.228301 for details on the polymers used in experiments.
[40] C. B. Muller and W. Richtering, Colloid Polym. Sci. **286**, 1215 (2008).
[41] See the Supplemental Material at http://link.aps.org/supplemental/10.1103/PhysRevLett.111.228301 for details on the FCS experimental methods.
[42] See the Supplemental Material at http://link.aps.org/supplemental/10.1103/PhysRevLett.111.228301 for details on the rheometry data and result analysis.
[43] T. Odijk, Biophys. J. **79**, 2314 (2000).
[44] See the Supplemental Material at http://link.aps.org/supplemental/10.1103/PhysRevLett.111.228301 for DLS results.
[45] J. H. Wang, J. Am. Chem. Soc. **73**, 510 (1951).
[46] T. Kalwarczyk, M. Tabaka, and R. Hołyst, Bioinformatics **28**, 2971 (2012).
[47] M. K. Daddysman and C. J. Fecko, J. Phys. Chem. B **117**, 1241 (2013).
[48] E. Dauty and A. Verkman, J. Biol. Chem. **280**, 7823 (2005).
[49] I. Neri, N. Kern, and A. Parmeggiani, Phys. Rev. Lett. **110**, 098102 (2013).
[50] H. Hess and V. Vogel, Rev. Mol. Biotech. **82**, 67 (2001).